Power losses and windings temperature of an induction machine under voltage subharmonics

Piotr Gnaciński, Marcin Pepliński✉, Damian Hallmann

Gdynia Maritime University, Faculty of Electrical Engineering
Department of Marine Electrical Power Engineering
81-87 Morska St., 81-225 Gdynia, Poland
e-mail: {p.gnacinski; m.peplinski; d.hallmann}@we.umg.edu.pl
✉ corresponding author

Abstract
This paper deals with the effect of voltage subharmonics on power losses and heating of an induction motor. An increase in power losses in stator and rotor windings and their impact on windings temperature is presented for subharmonics of various frequencies. The results of this study's investigations are provided for subharmonics occurring as a single power quality disturbance and combined with voltage deviation. The appropriate electromagnetic computations were performed with the finite element method, and thermal ones – with an analytical method.

Introduction

In a power system, miscellaneous power quality disturbances occur, exerting a noxious effect on various elements, including induction motors (de Abreu & Emanuel, 2002; Tennakoon, Perera & Robinson, 2008; Gnaciński, 2009; Sürgevil & Akpnar, 2009; Emanuel, Langella & Testa, 2010; Zhao, Ciufo & Perera, 2014; Ghaseminezhad, Doroudi & Hosseinian, 2016; Gnaciński & Pepliński, 2016; Ghaseminezhad et al., 2017a; 2017b; Gonzalez-Cordoba et al., 2017; Zhao et al., 2017; Ghaseminezhad et al., 2019; Gnaciński, Hallmann & Pepliński, 2018; Zhang, An & Wu, 2018; Gnaciński et al., 2019). One of the most detrimental power quality disturbances is voltage subharmonics (subsynchronous interharmonics) – voltage components of frequency less than the fundamental one. Voltage subharmonics disturb work of synchronous generators, light sources, transformers and control systems (Sürgevil & Akpnar, 2009; Emanuel, Langella & Testa, 2010). In induction machines, voltage subharmonics can result in the local saturation of a magnetic circuit, fluctuations of electromagnetic torque and rotational speed, an increase in currents and power losses, windings overheating, thermal loss of life and vibrations (de Abreu & Emanuel, 2002; Gnaciński, 2009; Sürgevil & Akpnar, 2009; Emanuel, Langella & Testa, 2010; Stumpf et al., 2010; Ghaseminezhad, Doroudi & Hosseinian, 2016; Ghaseminezhad et al., 2017a; 2017b; Ghaseminezhad et al., 2019; Gnaciński, Hallmann & Pepliński, 2018; Gnaciński et al., 2019). It should be noted that even seemingly inconsiderable subharmonic contamination may exert a harmful effect on induction motors. For example, according to de Abreu & Emanuel (2002), a voltage subharmonic of value and frequency equal to 0.25% and 10% of the fundamental voltage component, could reduce the operational life of 100-HP induction machine by 17%. Further, a voltage subharmonic of value 0.2% may result in excessive vibration level (Gnaciński et al., 2019).

Voltage subharmonics originate from work of non-linear receivers, such as arc furnaces and

inverters (Bolen & Gu, 2006; Sürgevil & Akpnar, 2009; Basic, 2010; Soltani et al., 2017; Soltani et al., 2018). They are also produced by renewable sources of energy (Bolen & Gu, 2006; Agrawal, Mohanty & Agarwal, 2015; Karimi et al., 2016; Kovaltchouk et al., 2016; Xie et al., 2017; Elwira-Ortiz et al., 2918). Additionally, significant values of subharmonics can occur in the output voltage of some inverters (Stumpf et al., 2010; Stumpf, Jardan & Nagy, 2012). It should be noted that periodically voltage fluctuations are interconnected with the presence of subharmonics and interharmonics (Tennakoon, Perera & Robinson, 2008). Voltage fluctuations are caused by renewable sources of energy and work of high-power loads such as arc furnaces, rolling mills and railway traction (Bolen & Gu, 2006; Sürgevil & Akpnar, 2009; Xie et al., 2017). Furthermore, low power receivers may lead to voltage fluctuations (Bolen & Gu, 2006).

Although voltage subharmonics can have a harmful impact on various elements of a power system, power quality standard does not impose a limitation on them. For example, in the standard EN 50160 Voltage Characteristics of Electricity Supplied by Public Distribution Systems (EN 50160:2010) has the following statement regarding subharmonics (understood as subsynchronous interharmonics), and interharmonics as "the level of interharmonics is increasing due to the development of frequency converters and similar control equipment. Levels are under consideration, pending more experience." Therefore, there is a need to carry out an in-depth investigation concerning the harmfulness of voltage subharmonics. The results of investigations carried out on an induction machine under subharmonics were presented in (de Abreu & Emanuel, 2002; Gnaciński, 2009; Sürgevil & Akpnar, 2009; Emanuel, Langella & Testa, 2010; Stumpf et al., 2010; Ghaseminezhad, Doroudi & Hosseinian, 2016; Ghaseminezhad et al., 2017a; 2017b; Ghaseminezhad et al., 2019; Gnaciński, Hallmann & Pepliński, 2018; Gnaciński et al., 2019). However, none of these papers address the impact of voltage subharmonics on each power losses component. Moreover, the effect of each power losses component on windings temperature has not been analyzed. The purpose of this paper is to analysis power losses in stator and rotor windings under positive-sequence subharmonics and their impact on additional machine heating. The presented results of investigations are based on field electromagnetic computations and analytical thermal calculations. The scope of this study is limited to low-power totally enclosed fan-cooled cage induction motors driving loads of high inertia moment.

Electromagnetic model

Electromagnetic calculations were performed with the finite element method. The machine model was implemented in ANSYS Maxwell environment.

The numerical computations with finite element method are based on the solution of the time-dependent magnetic field and movement equations:

$$\nabla \times \upsilon \, \nabla \times A =$$

$$= J_s - \sigma \frac{\partial A}{\partial t} - \sigma \nabla V + \nabla \times H_c + \sigma v \times \nabla \times A \quad (1)$$

$$J\beta + T_{m\text{loss}} = T_e - T_l \quad (2)$$

where:
H_c – permanent magnet coercive,
v – velocity of moving part,
A – vector magnetic potential,
V – electric potential,
υ – reluctance,
J_s – source current density,
J – moment of inertia,
σ – electrical conductivity,
$T_{m\text{loss}}$ – torque corresponding to mechanical losses inside a machine,
T_e – electromagnetic torque,
T_l – load torque,
β – angular acceleration.

The applied mesh consists of roughly 22,000 elements (Figure 1). The model was identified for an induction cage machine type TSG 100L-4B, of rated power 3 kW, rated current – 6.9 A, rated rotational speed – 1415 rpm and moment of inertia – 0.0082 kg·m². It should be noted that this motor has comparatively strongly saturated magnetic circuit and is particularly sensitive to overvoltage.

In order to validate the model, the results of numerical calculations are compared with empirical
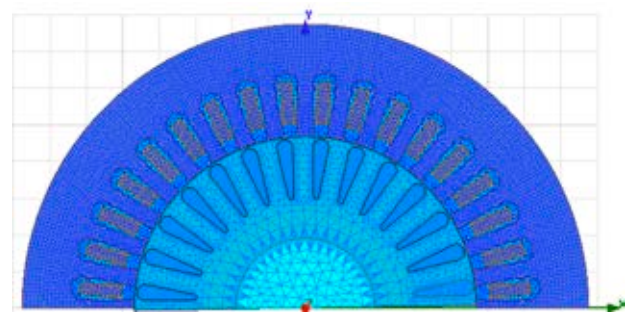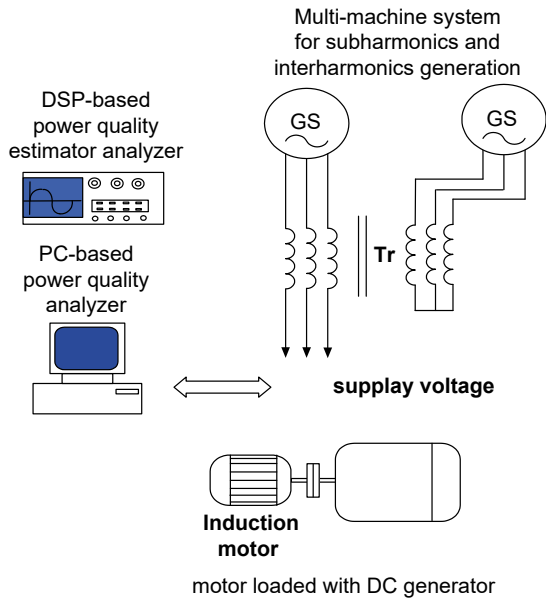

Figure 1. Applied mesh

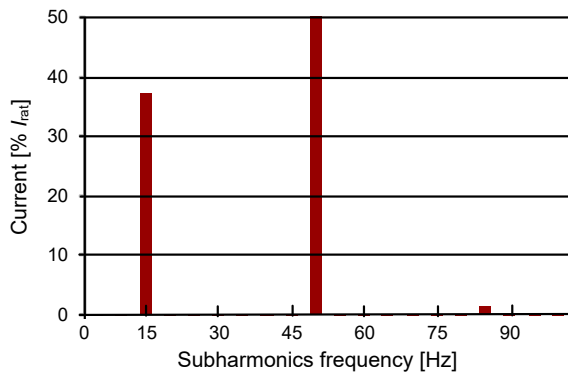**Figure 2. Simplified diagram of the measurement stand**

Figure 3. Spectrum of the supply current for voltage containing subharmonic of frequency 15 Hz and value 2.5% U_1, determined on the basis of FEM calculations. The frequency components are related to the rated current

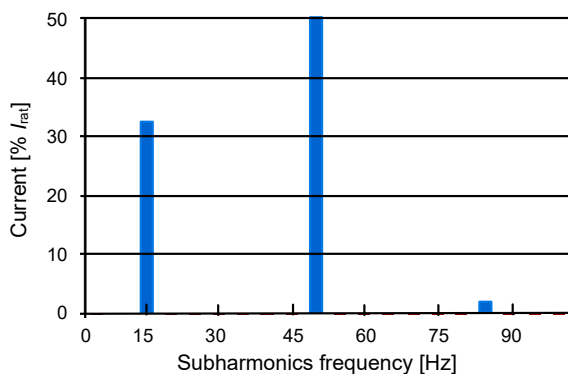**Figure 4. Spectrum of the supply current for voltage containing subharmonic of frequency 15 Hz and value 2.5% U_1, determined on the basis measurements. The frequency components are related to the rated current**

data. The measurement stand consists of the induction cage machine loaded with a DC generator, a multi-machine system for subharmonics and interharmonics generation based on (Ho & Fu, 2001) and power quality analyzers – a PC based one and a DSP-based power quality estimator-analyzer (Tarasiuk, 2011), worked out in Gdynia Maritime University for commercial purposes and certified by Polish Register of Shipping. The schematic of the laboratory stand is shown in Figure 2. Exemplary spectrums of the motor current under subharmonics, obtained on the basis of computations and measurements, are shown in Figures 3–6.
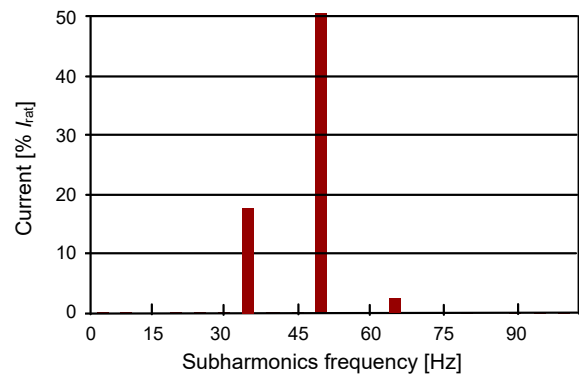

Figure 5. Spectrum of the supply current for voltage containing subharmonic of frequency 35 Hz and value 2.5% U_1, determined on the basis of FEM calculations. The frequency components are related to the rated current
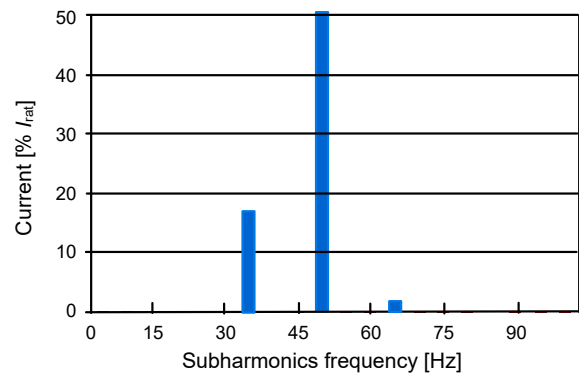

Figure 6. Spectrum of the supply current for voltage containing subharmonic of frequency 35 Hz and value 2.5% U_1, determined on the basis of measurements. The frequency components are related to the rated current

Thermal model

Let us denote the most exposed to overheating winding (under-voltage unbalance) as winding 1, and other windings – as winding 2 and winding 3. Under power quality disturbances and variation of the load torque, the steady-state temperature of end-windings (winding 1) of low-power, fully enclosed fan-cooled

cage induction motors can be estimated (Gnaciński, 2009; Gnaciński & Pepliński, 2016) as:

$$\Delta T_{w1} = w_0(1 + \Delta p_{w1}) +$$
$$+ \beta k_c \left(1 - w_0 + \sum_{i \neq 0} w_i \Delta p_i - w_0 \Delta p_{w1} \right) \qquad (3)$$

where:

$$\beta = \frac{1 - \alpha k_t}{1 - \alpha k_t k_c \left(1 + \dfrac{\sum\limits_{i \neq 0} w_i \Delta p_i - w_0 \Delta p_{w1}}{1 - w_0} \right)} \qquad (4)$$

$$\Delta p_i = \frac{\Delta P_i - \Delta P_{iN}}{\Delta P_{iN}} \qquad (5)$$

where:

ΔT_{w1} – the normalized maximal end windings temperature rise, that is a ratio of the end windings temperature rise in the hottest point, corresponding to the real working conditions and the nominal conditions ($\Delta \vartheta_{ew\text{nom}}$);

w_i – loss weight factors (Gnaciński, 2009) (LWL) – the assessed contribution of each power loss component to $\Delta \vartheta_{ew\text{nom}}$;

ΔP_i – power loss component in the working point;

ΔP_{iN} – each power loss component in the nominal work conditions;

Δp_{w1} – the relative increase in power losses described with (5), for copper losses occurring in *winding* 1;

k_c, k_t, w_0, α – coefficients described in (Gnaciński, 2009).

Eq. (2) describes the effect of variation of windings resistance on Joule losses, which leads to an additional increase in temperature.

A more detailed description of the applied thermal model, as well as a comparison of thermal calculations and thermal test, are provided in (Gnaciński 2009, Gnaciński & Pepliński, 2016).

For purposes of this paper, the increases in the following power losses components were taken into account: an increase in power losses in rotor windings (Δp_{Al}), stator windings (Δp_w), rotor iron (Δp_{rFe}) and stator iron (Δp_{Fe}). The mechanical losses were assumed constant. The values of loss weight factors were determined with the method presented in (Gnaciński, 2009) and given in Table 1 (partially based on (Gnaciński, 2009)).

On the grounds of (3), the contribution of the increase Δp_w in the end windings over-temperature
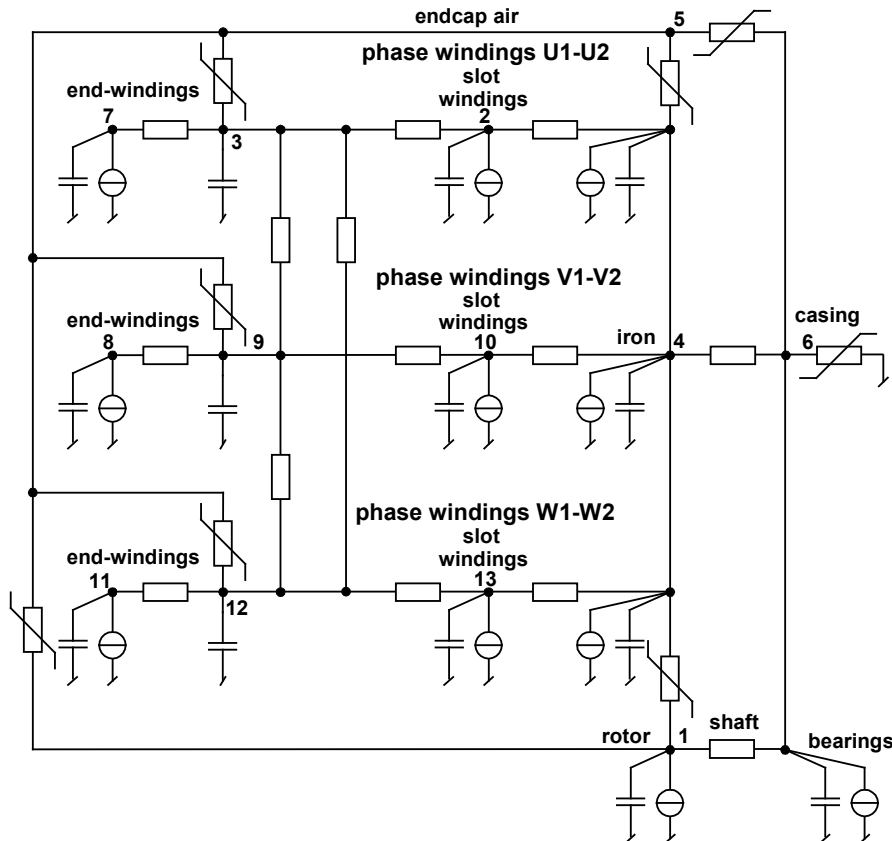

Figure 7. Applied equivalent thermal network

Table 1. Loss weight factors of the investigated induction machine type TSg 100L-4B

Description	Notation	Value
LWL of rotor windings	w_{Al}	0.17
LWL of rotor iron (including stray losses)	w_{rFe}	0.03
LWL of stator windings, including:	w_w	0.7
– LWL of *winding* 1	w_{w1}	0.39
– LWL of *winding* 2	w_{w2}	0.16
– LWL of *winding* 3	w_{w3}	0.16
LWL of stator iron (including stray losses)	w_{Fe}	0.08
LWL of mechanical losses	w_m	0.015

(caused by power quality disturbances) was assessed with the following expression:

$$\Delta\vartheta_{adw} = \Delta\vartheta_{ad} \frac{w_w \Delta p_w}{\sum_{i \neq 0} w_i \Delta p_i} \quad (6)$$

where:

$\Delta\vartheta_{ad}$ – the additional increase in end windings temperature rise, caused by power quality disturbances.

In analogical method, the contribution of the increase Δp_{Al} in $\Delta\vartheta_{ad}$ (denoted as $\Delta\vartheta_{ad\,Al}$) was estimated. For the paper purpose, the increase $\Delta\vartheta_{ad}$ was calculated on the basis of the electromagnetic field model presented in section 2 and an equivalent thermal network (Figure 7), described in (Gnaciński, Hallmann & Pepliński, 2018).

Results of investigations

Figures 8–11 present the results of investigations on power losses and heating of an induction machine under subharmonics. The appropriate computations were carried out for the load torque of its rated value, voltage subharmonic equal to 2% and the moment of load inertia corresponding to the moment of the DC generator coupled with the motor – that is for the moment of inertia 15 times larger than the motor moment.
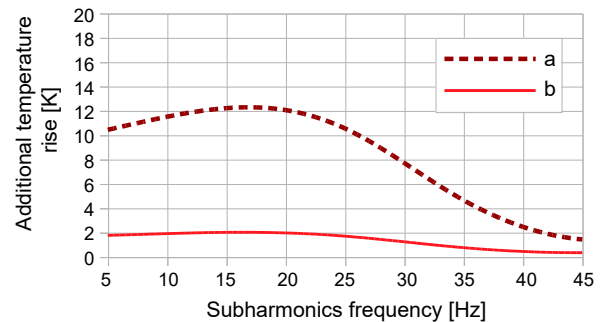
The increases in power losses in stator and rotor windings (Δp_w, Δp_{Al}, respectively) are shown in Figure 8, for the fundamental voltage component equal to U_{rat}. The maximal value of the increase Δp_w is about 15%, which corresponds to circa 50 W. Further, the increase in Δp_{Al} is up by roughly 20% (35 W). Both the increases reach the maximum for the frequency f_{sh} = 15–20 Hz, while for the frequency f_{sh} = 40 Hz they are below 5%. Analogical characteristics for 10% overvoltage combined with subharmonics are presented in Figure 9. Generally, overvoltage leads to a reduction in power losses in rotor windings.
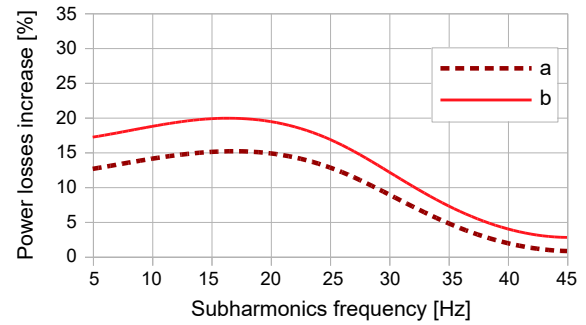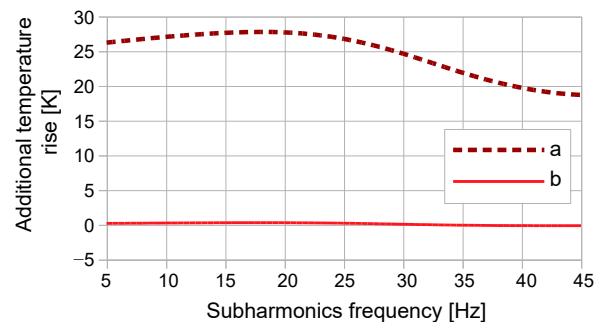

Figure 8. Percent increase in power losses caused by voltage subharmonic of value 2% U_{rat}; a – stator windings, b – rotor windings
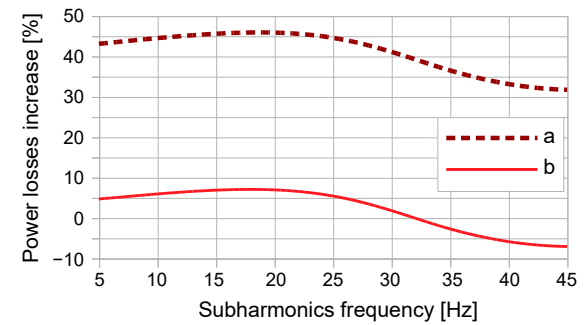
Figure 9. Percent increase in power losses caused by 10% overvoltage combined with voltage subharmonic of value 2% U_{rat}; a – stator windings, b – rotor windings

Figure 10. Contribution of each power losses component in an additional increase in windings temperature $\Delta\vartheta_{ad}$, caused by voltage subharmonic of value 2% U_{rat}; a – power losses in stator windings; b – power losses in rotor windings

Figure 11. Contribution of each power losses component in an additional increase in windings temperature $\Delta\vartheta_{ad}$, caused 10% overvoltage combined with voltage subharmonic of value 2% U_{rat}; a – power losses in stator windings; b – power losses in rotor windings

For this reason, the increase in Δp_{Al} is negative for some frequencies (Figure 9). Contrastingly, the increase in Δp_w is up to about 45% (Figure 9).

One could expect that the increase in end windings temperature due to an increase in stator windings power losses should be proportional to its value. Similarly, the increase in end windings temperature due to an increase in rotor power losses can be expected too also be proportional. In the previous section, the relative increases in end windings temperature due to an increase in power losses in windings and rotor are defined as contributions $\Delta\vartheta_{adw}$ and $\Delta\vartheta_{ad\ Al}$, respectively. Their values are presented in Figures 10 and 11 versus subharmonic frequency, for both considered supply conditions. For $U_1 = U_{rat}$ (Figure 10) the contribution $\Delta\vartheta_{adw}$ is up to 85% and for $U_1 = 110\%\ U_{rat}$ (Figure 11) is even greater. The contribution $\Delta\vartheta_{ad\ Al}$ does not exceed a dozen and so per-cent despite the fact that the increases in windings power losses and rotor power losses (expressed in watts) are of comparable values for $U_1 = U_{rat}$. The moderate effect of rotor power losses on stator windings temperature can be explained by the comparatively high value of thermal resistance between a stator and a rotor. In addition, some parts of heat occurring in the rotor flow out through endcap air to end shields and through a shaft. Consequently, the increase in stator windings power losses exerts a significantly greater effect on end windings temperature than the increase in rotor power losses of the same value.

In summary, for the power quality disturbances under consideration, the investigated machine is overheated mostly by the increase in power losses in stator windings despite the fact that subharmonics cause a comparable increase in power losses in rotor windings.

Conclusions

For the investigated machine, voltage subharmonics caused comparable increases in power losses in the stator and rotor windings. Further, in the voltage subharmonics combined with overvoltage, power losses in the rotor windings may be less than in nominal work conditions. For both the cases – voltage subharmonics occurring as a single power quality disturbance and combined with overvoltage – the reason why the machine overheated was almost exclusively because of an increase of power losses in stator windings.

The outcomes of this work should be useful for calculating the end-windings temperature of an induction machine supplied with voltage containing subharmonics. As power losses in rotor windings caused by subharmonics do not significantly affect stator windings temperature, rough assessment of this power losses component should not result in a decrease in accuracy of thermal calculations.

References

1. DE ABREU J.P.G. & EMANUEL, A.E. (2002) Induction motor thermal aging caused by voltage distortion and imbalance: loss of useful life and its estimated cost. *IEEE Transactions on Industry Applications* 38, 1, pp. 12–20.
2. AGRAWAL, S., MOHANTY, S.R. & AGARWAL, V. (2015) Harmonics and inter harmonics estimation of DFIG based standalone wind power system by parametric techniques. *International Journal of Electrical Power & Energy Systems* 67, pp. 52–65.
3. BASIC, D. (2010) Input current interharmonics of variable-speed drives due to motor current imbalance. *IEEE Transactions on Power Delivery* 25, 4, pp. 2797–2806.
4. BOLEN, M.H.J. & GU, I.Y.H. (2006) *Signal processing of power quality disturbances*. New York: Wiley.
5. ELVIRA-ORTIZ, D.A., OSORNIO-RIOS, R.A., MORINIGO-SOTELO, D., ROSTRO-GONZALEZ, H. & ROMERO-TRONCOSO, R.J. (2018) *Power quality monitoring system under different environmental and electric conditions*. In: Harmonics and Quality of Power (ICHQP), 18th International Conference on IEEE, pp. 1–6, doi:10.1109/ICHQP.2018.8378846.
6. EMANUEL, A.E., LANGELLA, R. & TESTA, A. (2010) Limiting low frequency interharmonic distortion and voltage fluctuations. *IEEE Power and Energy Society General Meeting*, pp. 1–6, doi:10.1109/PES.2010.5589809.
7. EN 50160:2010. *Voltage characteristics of electricity supplied by public distribution network*.
8. GHASEMINEZHAD, M., DOROUDI, A. & HOSSEINIAN, S.H. (2016) Double-Cage Induction motors behavior under Flicker Conditions. *Journal of Electric Power & Energy Conversion Systems* 1, 1, pp. 1–7.
9. GHASEMINEZHAD, M., DOROUDI, A., HOSSEINIAN, S.H. & JALILIAN, A. (2017a) Analysis of voltage fluctuation impact on induction motors by an innovative equivalent circuit considering the speed changes. *IET Generation, Transmission & Distribution* 11(2), pp. 512–519.
10. GHASEMINEZHAD, M., DOROUDI, A., HOSSEINIAN, S.H. & JALILIAN, A. (2017b) An Investigation of Induction Motor Saturation under Voltage Fluctuation Conditions. *Journal of Magnetics* 22(2), pp. 306–314.
11. GHASEMINEZHAD, M., DOROUDI, A., HOSSEINIAN, S.H. & JALILIAN, A. (2019) Investigation of Increased Ohmic and Core Losses in Induction Motors Under Voltage Fluctuation Conditions. *Iranian Journal of Science and Technology, Transactions of Electrical Engineering* 43, pp. 373–382.
12. GNACIŃSKI, P. (2009) Effect of power quality on windings temperature of marine induction motors. Part I. Machine model. *Energy Conversion and Management* 50 (10), pp. 2463–2476.
13. GNACIŃSKI, P., HALLMANN, D. & PEPLIŃSKI, M. (2018) *Cage induction machine under voltage subharmonics combined with voltage deviation*. In: Proc. of XXIIIrd International Conference on Electrical Machine, Ramada Plaza Thraki, Alexandroupoli – Greece, pp. 1095–1100, September 3–6, 2018.

14. Gnaciński, P. & Pepliński, M. (2016) Lowered voltage quality and load-carrying capacity of induction motors. *IET Electric Power Applications* 10.9, pp. 843–848.

15. Gnaciński, P., Pepliński, M., Murawski, L. & Szeleziński, A. (2019) Vibration of Induction Machine Supplied with Voltage Containing Subharmonics and Interharmonics. *IEEE Transactions on Energy Conversion* 34, 4, pp. 1928–1937.

16. Gonzalez-Cordoba, J.L., Osornio-Rios, R.A., Granados-Lieberman, D., Romero-Troncoso, R. De J. & Valtierra-Rodriguez, M. (2017) Correlation model between voltage unbalance and mechanical overload based on thermal effect at the induction motor stator. *IEEE Transactions on Energy Conversion* 32(4), pp. 1602–1610.

17. Ho, S.L. & Fu, W.N. (2001) Analysis of indirect temperature-rise tests of induction machines using time stepping finite element method. *IEEE Transactions on Energy Conversion* 16, 1, pp. 55–60.

18. Karimi, M., Mokhlis, H.,Naidu, K., Uddin, S. & Bakar, A.H.A. (2016) Photovoltaic penetration issues and impacts in distribution network – A review. *Renewable and Sustainable Energy Reviews* 53, pp. 594–605.

19. Kovaltchouk, T., Armstrong, S., Blavette, A., Ahmed, H.B. & Multon, B. (2016) Wave farm flicker severity: Comparative analysis and solutions. *Renewable Energy* 91, pp. 32–39.

20. Soltani, H., Davari, P., Zare, F. & Blaabjerg, F.(2018) Effects of modulation techniques on the input current interharmonics of Adjustable Speed Drives. *IEEE Transactions on Industrial Electronics* 65, 1, pp. 167–178.

21. Soltani, H., Davari, P., Zare, F., Loh, P.C. & Blaabjerg, F. (2017) Characterization of input current interharmonics in adjustable speed drives. *IEEE Transactions on Power Electronics* 32, 11, pp. 8632–8643.

22. Stumpf, P., Jardan, R.K. & Nagy, I. (2012) Subharmonics generated by space vector modulation in ultrahigh speed drives. *IEEE Transactions on Industrial Electronics* 59, 2, pp. 1029–1039.

23. Stumpf, P., Varga, Z., Sepsi, T.D., Jardan, R.K. & Nagy, I. (2010) *Ultrahigh speed induction machine overheated by subharmonics of PWM inverter*. In: Proceedings IEEE 36th Annual Conference of the IEEE Industrial Electronics Society, pp. 1754–1759, doi:10.1109/IECON.2010.5675416.

24. Sürgevil, T. & Akpnar, E. (2009) *Effects of electric arc furnace loads on synchronous generators and asynchronous motors*. In: Proceedings of International Conference on Electrical and Electronics Engineering, pp. I-49–I-53.

25. Tarasiuk, T. (2011) Estimator-analyzer of power quality: Part I – Methods and algorithms. *Measurement: Journal of the International Measurement Confederation* 44, 1, pp. 238–247.

26. Tennakoon, S., Perera, S. & Robinson, D. (2008) Flicker attenuation – Part I: Response of three-phase induction motors to regular voltage fluctuations. *IEEE Transactions on Power Delivery* 23, 2, pp. 1207–1214.

27. Xie, X., Zhang, X., Liu, H., Liu, H., Li, Y. & Zhang, C. (2017) Characteristic Analysis of Subsynchronous Resonance in Practical Wind Farms Connected to Series-Compensated Transmissions. *IEEE Transactions on Energy Conversion* 32(3), pp. 1117–1126.

28. Zhang, D., An, R. & Wu, T. (2018) Effect of voltage unbalance and distortion on the loss characteristics of three-phase cage induction motor. *IET Electric Power Applications* 12, 2, pp. 264–270.

29. Zhao, K., Cheng, L., Zhang, C., Nie, D. & Cai, W. (2017) Induction motors lifetime expectancy analysis subject to regular voltage fluctuations. *IEEE Electrical Power and Energy Conference (EPEC)*, pp. 1–6, doi:10.1109/EPEC.2017.8286230.

30. Zhao, K., Ciufo, P. & Perera, S. (2014) *Performance of adjustable speed drives subject to regular voltage fluctuations*. Proceedings of International Conference on Harmonics and Quality of Power, ICHQP, pp. 253–257, doi:10.1109/ICHQP.2014.6842863.